Preprints of the 21st IFAC World Congress (Virtual)
Berlin, Germany, July 12-17, 2020

A fatigue-oriented cost function for optimal individual pitch control of wind turbines

David Collet [*,**] **Mazen Alamir** [**] **Domenico Di Domenico** [*]
Guillaume Sabiron [*]

[*] *IFPEN, Solaize, France (e-mail: david.collet@ifpen.fr, domenico.didomenico@ifpen.fr, guillaume.sabiron@ifpen.fr).*
[**] *GIPSA-Lab, CNRS, and University of Grenoble Alpes, Saint-Martin d'Hères, France (e-mail: mazen.alamir@grenoble-inp.fr)*

Abstract: In a context of wind power production growth, it is necessary to optimize the levelized cost of energy by maximizing the profit of operating wind turbines, which is defined as the difference between gains (e.g. energy sold) and losses (e.g. operation and maintenance cost). Operation and maintenance cost is intimately related to fatigue damage. However, considering fatigue directly in an optimization needs to be carefully done because its faithful model does not fit standard forms. In this paper, it is first shown that the variance of a signal and its corresponding damage using fatigue theory are nonlinearly related. Therefore, this relationship is used to design a convex cost function approximating fatigue. Preliminary tests suggest promising results regarding the relevance of this formulation in optimizing fatigue trade-off when compared to a family of quadratic cost functions. The proposed formulation allows to directly consider economic parameters in the cost function, limiting thus the sensitivity to parameter tuning.

Keywords: Optimal control, Optimization, Fatigue, Wind turbines, Individual Pitch Control.

1. INTRODUCTION

Wind energy production has been exponentially growing in the last decades, with about 591 GW globally installed in 2018 compared with 94 GW in 2007, see GWEC (2018). In order to achieve COP21 objective, which is to maintain CO_2 emissions below 5.4×10^{12} kilograms per year, the wind energy industry is expected to develop even further, see GWEC (2016). This energetic transition requires a large economic investment. It is thus necessary to optimize Horizontal Axis Wind Turbine (HAWT) operation and maintenance cost.
Control of HAWT blade pitch angle can contribute to this challenge. The main objectives of HAWT blade pitch control are to regulate output power and rotor speed while reducing mechanical fatigue. In the early work on blade pitch control, wind was assumed to be uniformly distributed over the rotor area. Therefore, all the blades were pitched to the same angle, this technique is called Collective Pitch Control (CPC). With recent increase in rotor diameter, this assumption is less and less valid. Aerodynamic forces on the blades fluctuate with the azimuth angle while the blade pitch angle remains constant, see Hansen (2015). Therefore, by varying each blade pitch angle individually depending on its azimuth, blades fatigue loads can be alleviated. This technique is called Individual Pitch Control (IPC), see Bossanyi (2003).
IPC is usually divided in two stages:

(1) The CPC stage whose objective is to regulate the rotor rotational speed and power, while alleviating the fatigue loads on the tower.
(2) The IPC stage that gives a differential pitch angle on each blade, added to the collective pitch angle, in order to reduce the unbalanced loads on the rotor, contributing to the rotating components damage (i.e. blades, rotor bearing, blade bearings)

Therefore, the goal of the IPC stage is essentially to optimize the trade-off between the fatigue damage of various components, in order to minimize the HAWT operating cost.
Optimal control is a good solution to achieve this objective. However, expressing this objective as an economic cost function for optimal control is a challenging task due to the fatigue damage estimation, see Hammerum et al. (2007) and Barradas-Berglind and Wisniewski (2016). Fatigue damage is quantified using the Palmgrem-Miner fatigue theory, where it is expressed as a sum of damages caused by hysteresis load cycles, see Palmgren (1924). These cycles are counted using a RainFlow Counting (RFC) algorithm (see Downing and Socie (1982)) which cannot be expressed as a simple algebraic function. Consideration of fatigue as an explicit control objective remains an open topic, see Knudsen et al. (2015). To our best knowledge, it is possible to find in the literature four methods considering directly fatigue as an objective cost function for HAWT control:

(1) In Hammerum et al. (2007), the spectral properties of the stress history are used to design an optimal feedback controller.
(2) In Collet et al. (2019), a data driven surrogate model is designed to predict fatigue from wind spectrum

characteristics and controller. This surrogate model is used to select the best controller among several candidates.

(3) In de Jesus Barradas-Berglind et al. (2015), a quadratic cost function parameters are varied to match an on-line estimated economic fatigue cost function.

(4) In Loew et al. (2019), a sequential optimization is made where the cost function parameters are iteratively modified between gradient steps, based on RFC.

The two last methods are different from the others because they are using a temporal approach instead of a spectral one. These approaches are both used to define an objective cost function for Model Predictive Control (MPC). They are then compared to a classical MPC, using quadratic norms as objective cost function.

This paper approach bridges several aspects of the above methods. It uses a data-driven surrogate model relating quadratic norms (variance) and fatigue of given signals, in order to approximate a fatigue trade-off objective cost function. This approximated objective cost function is used to optimize the system input trajectory. It is different from the second method, as the surrogate model relates trajectory time series to fatigue damage, instead of wind characteristics to fatigue. It differs also from the fourth method, as a global differentiable cost function is derived and used avoiding the use of RFC in the MPC.

The outline of this paper is the following. Fatigue theory is presented in Section 2. Then, in Section 3, the novel fatigue-oriented cost function is introduced. In Section 4, an example of application on HAWT (IPC) is depicted along with the parametrization of a quadratic cost function. Afterwards, the performance of fatigue-oriented optimization is compared to the quadratic one in Section 5.3. Eventually, a conclusion along with an outlook on the undergoing work is given in Section 6.

2. FATIGUE ESTIMATION

It is possible to estimate the fatigue damage endured by one component using the Palmgren-Miner linear damage rule, see Palmgren (1924) and Miner (1945). In fatigue theory, it is considered that any material contains cracks, and these cracks propagate inside the material during its lifetime, until it fails. To propagate a crack, only the value of the load at reversals matter, therefore fatigue expression is not an integral over time and load history must be post-processed using the Downing-Socie RainFlow Counting (RFC) algorithm, see Downing and Socie (1982). This algorithm can be considered as a functional yielding from a load history $\mathcal{H}$, the number of occurrences n_s of hysteresis cycles s of range L_s^R and mean L_s^m:

$$\text{RFC} : \mathcal{H} \longrightarrow (n_s, L_s^R, L_s^m) \tag{1}$$

Each hysteresis cycle contributes to a certain amount of damage. Summing these damages allows to estimate the total damage endured by one component denoted by D, expressed as follows:

$$D = \sum_{s=1}^{M} \frac{n_s}{N(L_s^R, L_s^m)} \tag{2}$$

where M is the number of different kinds of cycles counted in the RFC algorithm, $N(.,.)$ is a function of the load cycle amplitude, yielding the number of cycles to failure of range L_s^R and mean L_s^m that the material can endure throughout its lifetime. It should be noticed that the material is not damaged when $D = 0$ and it fails when $D \geq 1$. The expression of $N(\cdot,\cdot)$ is the following:

$$N(L_s^R, L_s^m) = \left(\frac{L^{ult} - L_s^m}{L_s^R} \right)^m \tag{3}$$

where m is the Wöhler exponent, varying from one material to another (for instance, $m = 4$ for steel and $m = 10$ for glass fiber). L^{ult} is the ultimate design load, the maximum load that the component can support. Assuming that the signal oscillates around zero, it is possible to neglect the so called Goodman correction (see Hayman (2012)) and consider that $L_s^m = 0 \ \forall s$. Therefore the ultimate design load becomes a multiplicative factor of the fatigue damage.

3. A NOVEL FATIGUE-ORIENTED COST FUNCTION

In this section, the fatigue trade-off objective function is first introduced. Then the relationship between variance and fatigue is presented, and eventually the novel fatigue-oriented cost function is derived.

3.1 Fatigue trade-off objective function

This paper aims at defining a control framework for the optimization of the fatigue damage trade-off between various HAWT components. One way to express this objective in an economic cost function is to weight each component fatigue damage by their respective economic costs, as follows:

$$J_{\text{fat}}(\mathbf{y}) = \sum_{i=1}^{n} \pi_i D(\mathbf{y}_i) \tag{4}$$

where J_{fat} is the total economic cost of fatigue, $\mathbf{y}$ is the system output trajectory, n is the number of HAWT components considered, $D(.)$ is a function that yields the fatigue damage from a load history, π_i and $\mathbf{y}_i$ are respectively the i^{th} component economic cost and output trajectory. However, due to the incorporation of RFC algorithm in fatigue damage estimation, the expression of the cost function J_{fat} is non algebraic and discontinuous. This makes the optimization problem difficult to solve and motivate the search for a differentiable representation.

3.2 Relationship between variance and fatigue

Using a quadratic cost function as objective in the formulation of optimization problems is usually desirable, as it is differentiable, convex, and makes the optimization relatively simple. Moreover, quadratic cost functions are generally suitable to represent energy cost in many areas. A quadratic cost is denoted by J_{quad}:

$$J_{\text{quad}}(\mathbf{y}, \mathbf{u}) = \sum_{k=1}^{N} y(t_k)^T Q y(t_k) + u(t_k)^T R u(t_k) \tag{5}$$

where $\mathbf{u}$ is the system output trajectory, N is the discrete prediction horizon length, t_k is the k^{th} time instant,

$y = (y_1 \ \dots \ y_n)^T$ is the vector of the system instantaneous outputs, u is the vector of the system instantaneous inputs, Q and R are semi-definite positive matrices of appropriate dimensions. However, a quadratic cost function does not quantify fatigue damage as mentioned in Knudsen et al. (2015). In de Jesus Barradas-Berglind et al. (2015), it is suggested that there exists matrices Q and R such that J_{quad} approximates J_{fat}. It also suggests that the values of these matrices are adapted online and are thus time varying. In Biegel (2011), it is observed that the relationship between quadratic cost functions and fatigue is monotonically increasing and strongly nonlinear. Therefore minimizing the variance of one signal is equivalent to minimizing its damage. However, as the relationship is nonlinear, minimizing a linear combination of variances is not equivalent to minimizing the same linear combination of damages.

In this paper, this study is pursued further by plotting the relationship between quadratic cost functions and fatigue in the logarithmic space (see Fig. 1). Stress histories are generated from gaussian noise filtered through first order filters, whose time constant and static gain are randomly drawn in uniform distribution on the respective intervals $[1, 10]$ (in seconds) and $]0, 100]$, instead of output signals from a HAWT simulator as in the previously cited study. This choice was made in order to generate rapidly a bigger dataset, allowing thus to have a relevant and robust regression. In Fig. 1, for each stress history $\mathcal{H}_i$, a couple $(\text{Var}(\mathcal{H}_i), \mathcal{D}(\mathcal{H}_i))$ is obtained and plotted. The variance, denoted by Var, is computed using its discrete expression:

$$\text{Var}(\mathbf{z}) = \frac{1}{N}\sum_{i=1}^{N} z(t_k)^2 - \left(\frac{1}{N}\sum_{i=1}^{N} z(t_k)\right)^2 \tag{6}$$

where z is a signal whose trajectory on the time interval under consideration is denoted by $\mathbf{z}$. The fatigue damage, denoted by $\mathcal{D}$, is estimated using RFC and the Palmgrem-Miner rule, the Goodman correction is neglected as stress histories oscillate around zero and L^{ult} is normalized to 1. It can be seen that there is a linear relationship between the logarithms of Var and $\mathcal{D}$. Using a linear regression, it is thus possible to approximate the fatigue damage $\mathcal{D}$ of the load history $\mathcal{H}_i$ from its variance Var:

$$\mathcal{D}(\mathcal{H}_i) \simeq \frac{e^b}{{L^{ult}}^m}\text{Var}(\mathcal{H}_i)^a \tag{7}$$

where a and b are respectively the proportional coefficient and intercept of the linear regression. From the regression it results that (a, b) are equal to $(2.6, 4.6)$ and $(5.6, 15.6)$ for, respectively, Wöhler coefficients of 4 and 10. In Fig. 2, the scatter plot of the ground truth and predicted fatigue using expression (7) shows that good approximations can be obtained.

3.3 The fatigue-oriented cost function

The insight of this work is to incorporate the relationship between variance and fatigue damage in the cost function. Therefore, the fatigue-induced cost function J_{fat} can be approximated by $\tilde{J}_{\text{fat}}$ given by:

$$\tilde{J}_{\text{fat}}(\mathbf{y}) = \sum_{i=1}^{n} \frac{\pi_i e^{b_i}}{{L_i^{ult}}^{m_i}} \left(\text{Var}(y_i)\right)^{a_i} \tag{8}$$

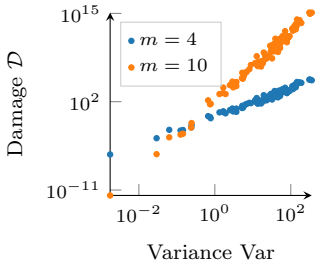

Fig. 1. Relation between variance Var and damage $\mathcal{D}$ in the logarithmic space, for two values of the Wöhler coefficient .

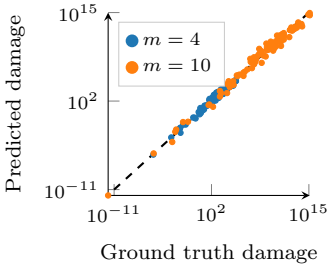

Fig. 2. Scatter plot of the ground truth damage and the predicted damage using the fatigue-oriented cost function.

where a_i and b_i are the regression's coefficients mentioned above and related to the output trajectory y_i.

The cost function $\tilde{J}_{\text{fat}}$ is particularly interesting for optimal control problems because it is a convex differentiable algebraic function, since the variance is a convex function and $a_i \geq 1 \ \forall i$. Therefore, there is no loss of convexity nor differentiability. Moreover the resulting problem can be solved directly using standard nonlinear programming solvers.

4. APPLICATION

The relevance of the fatigue-oriented cost function presented above must be compared to a family of quadratic cost function on a given system. This section first presents the system used for the comparison, before presenting the considered ensemble of quadratic cost functions. Eventually, the tuning procedure of the quadratic cost function is detailed, and some details on the optimizations are given.

4.1 System

A HAWT is a multi-body system, disturbed by the wind, whose different bodies vibrations are coupled. A HAWT is a multi-inputs/multi-outputs system, that can be simulated using high fidelity nonlinear aero-elastic HAWT simulators, such as FAST, see Jonkman et al. (2009). It can be noted that FAST allows to linearize the nonlinear equations modeling the HAWT behavior for control purposes. In this study, the focus is set on the IPC stage of a HAWT blade pitch controller. As mentioned previously, the IPC stage objective is to reduce the fatigue of various HAWT components. Therefore, the model of interest obtained from FAST linearization relates the blade pitch angles, the hub-height wind velocity and the out-of-plane blade root bending moments, denoted respectively by θ_i, v and M_i for blade i. The model is linearized around an operating point, defined by its collective blade pitch angle θ_{col}, steady wind velocity v_0, steady out-of-plane blade root bending moment M_0 and the azimuth angle $\psi(t)$. The linearized model is thus Linear Time Varying (LTV) and expressed as follows:

$$\begin{aligned} \dot{x} &= A(\psi(t))x + B(\psi(t))\delta\Theta + B_d(\psi(t))\delta v \\ \delta M &= C(\psi(t))x + D(\psi(t))\delta\Theta + D_d(\psi(t))\delta v \end{aligned} \tag{9}$$

where $\delta\Theta = [\delta\theta_1, \delta\theta_2, \delta\theta_3]^T$ are the three differential blade pitch angles with $\delta\theta_i = \theta_i - \theta_{col}$, $\delta M = [\delta M_1, \delta M_2, \delta M_3]^T$

are the three differential out of plane blade root bending moments with $\delta M_i = M_i - M_0$, $\delta v = v - v_0$ is the differential wind speed. The Coleman transform, denoted by $T(\psi)$ is defined as follows, see Coleman and Feingold (1957):

$$T(\psi) = \frac{2}{3}\begin{bmatrix}\cos(\psi) & \cos(\psi+\frac{2\pi}{3}) & \cos(\psi+\frac{4\pi}{3})\\ \sin(\psi) & \sin(\psi+\frac{2\pi}{3}) & \sin(\psi+\frac{4\pi}{3})\end{bmatrix} \quad (10)$$

This transform is classically used in the IPC literature to project states expressed in a rotating frame of coordinates onto a fixed frame of coordinates, see Bir (2008). As a corollary, the LTV model becomes Linear Time Invariant (LTI):

$$\begin{aligned}\dot{\tilde{x}} &= \tilde{A}\tilde{x} + \tilde{B}\tilde{\Theta} + \tilde{B}_d\delta v\\ \tilde{M} &= \tilde{C}\tilde{x} + \tilde{D}\tilde{\Theta} + \tilde{D}_d\delta v\end{aligned} \quad (11)$$

where $\tilde{\Theta} = T(\psi)\delta\Theta = [\theta_{yaw}, \theta_{tilt}]^T$ and $\tilde{M} = T(\psi)M = [M_{yaw}, M_{tilt}]^T$ are respectively the blade pitch angles and out-of-plane blade root bending moments expressed in the fixed frame of coordinates.
It is also considered that blade pitch actuators have the same first order dynamic, expressed as follows:

$$\tau\dot{\Theta} + \Theta = \Theta_{sp} \quad (12)$$

where Θ_{sp} is the setpoint angle for the actuator and τ is the actuator characteristic time. Then the Coleman transform must also be applied to (12), in order to extend the system expressed in (11). The actuator dynamic equation in the Coleman transform yields:

$$\dot{\tilde{\Theta}} = \Gamma\tilde{\Theta} + \tilde{\Theta}_{sp} \quad (13)$$

where $\tilde{\Theta}_{sp} = T(\psi)\Theta_{sp}$ and $\Gamma = \begin{bmatrix}-\frac{1}{\tau} & -\omega\\ \omega & -\frac{1}{\tau}\end{bmatrix}$ with ω the rotor rotational velocity. Then considering the state $\bar{x} = [\tilde{x}, \tilde{\Theta}]^T$, it is possible to merge the systems (11) and (13) to get:

$$\begin{aligned}\dot{\bar{x}} &= \bar{A}\bar{x} + \bar{B}\tilde{\Theta}_{sp} + \bar{B}_d\delta v\\ \bar{y} &= \bar{C}\bar{x} + \bar{D}\tilde{\Theta}_{sp} + \bar{D}_d\delta v\end{aligned} \quad (14)$$

where $\bar{y} = [\tilde{M}, \tilde{\Theta}]^T = [M_{yaw}, M_{tilt}, \theta_{yaw}, \theta_{tilt}]$.
In the following, the control objective is to optimize a trade-off between the fatigue of these four outputs, corresponding to the rotor bearing, shaft and blade pitch actuators. The parameters used for fatigue estimation are carefully chosen in order to yield a realistic fatigue trade-off and summarized in Table 1.

Table 1. Summary of the parameters used for the fatigue estimation, i corresponds to the output number.

i	L_i^{ult}	π_i	m_i
1	3×10^3	10^3	10
2	3×10^3	10^3	10
3	6.98×10^{-1}	1	4
4	6.98×10^{-1}	1	4

4.2 Quadratic cost function parametrization

In order to design a controller that optimizes the fatigue trade-off cost J_{fat} using a quadratic cost function, it is required to find matrices Q and R allowing to approximate J_{fat}. Therefore, the trial and error method consists in testing matrices Q and R values successively, and keep the one giving the minimum J_{fat}. Unfortunately, the symmetric matrices Q and R depend respectively on $\frac{p(p+1)}{2}$ and $\frac{m(m+1)}{2}$ variables, where p and m are respectively the system number of inputs and outputs. For the system (14), it makes 13 variables to tune, which can be computationally expensive.
However, in the specific test case of a three bladed wind turbine rotor, each blade is independent from each other in the rotating frame of coordinates. Therefore only the diagonal terms of the matrices need to be considered. Moreover, it can also be assumed that as all the blades and blade pitch actuators are identical, the same weights should be given to each blade pitch actuator and its corresponding blade root bending moments. Therefore, for the system presented in (9), the Q and R matrices can be parametrized as follows:

$$Q(\rho) = \rho I_3 \quad , \quad R = I_3 \quad (15)$$

where $\rho \in \mathbb{R}^+$ is a weight on the blade root bending moments and I_n is the identity matrix of dimension n. However, in the studied case of system (14), the outputs are the yawing and tilting blade root bending momentsand pitch angles. Therefore, due to the Coleman transform and the state vector extension, the parametrized matrices $\bar{Q}$ and $\bar{R}$ are considered:

$$\bar{Q}(\rho) = \begin{pmatrix}\rho I_2 & 0\\ 0 & I_2\end{pmatrix} \quad , \quad \bar{R} = \varepsilon I_2 \quad (16)$$

where $\varepsilon \ll \min(\rho, 1)$ is constant, such that the variations of blade pitch angles set-points do not impact the fatigue trade-off. Therefore, the quadratic cost J_{quad} depends on the system (14) outputs and inputs trajectories, denoted respectively by $\bar{\mathbf{y}}$ and $\tilde{\mathbf{\Theta}}_{\mathbf{sp}}$, and ρ:

$$J_{\text{quad}}(\bar{\mathbf{y}}, \tilde{\mathbf{\Theta}}_{\mathbf{sp}}, \rho) = \sum_{i=1}^{N} \bar{y}_k^T\bar{Q}(\rho)\bar{y}_k + \tilde{\Theta}_{sp,k}^T\bar{R}\tilde{\Theta}_{sp,k} \quad (17)$$

where $\bar{y}_k$ and $\tilde{\Theta}_{sp,k}$ are respectively the system (14) k^{th} instant outputs and inputs.

4.3 Parametrized quadratic cost function tuning procedure

The quadratic cost (17) is a function of $\bar{\mathbf{y}}$, $\tilde{\mathbf{\Theta}}_{\mathbf{sp}}$ and ρ. As $\bar{\mathbf{y}}$ is the output trajectory of the dynamic system (14), $\bar{\mathbf{y}}$ is a function of the initial state $\bar{x}_0$, the disturbance trajectory $\mathbf{v}$ and the input trajectory. This cost function is used in the following unconstrained optimization problem:

$$\begin{aligned}\min_{\tilde{\mathbf{\Theta}}_{\mathbf{sp}}} \quad & J_{\text{quad}}(\bar{\mathbf{y}}, \tilde{\mathbf{\Theta}}_{\mathbf{sp}}, \rho)\\ \text{s.t.} \quad & \bar{\mathbf{y}} = \bar{\mathbf{y}}(\bar{x}_0, \mathbf{v}, \tilde{\mathbf{\Theta}}_{\mathbf{sp}})\end{aligned} \quad (18)$$

where $\bar{x}_0$, $\mathbf{v}$ and ρ are given. Therefore, the solution of the above mentioned optimization problem is a function of $\bar{x}_0$, $\mathbf{v}$ and ρ and as a consequence, the system output trajectory $\bar{\mathbf{y}}$ and the fatigue cost J_{fat} at the optimum of the parametrized quadratic optimization are also function of $\bar{x}_0$, $\mathbf{v}$ and ρ.
For a given x_0 and $\mathbf{v}$, the tuning procedure of the quadratic cost function can thus be expressed as the following optimization problem:

$$\min_{\rho} \quad J_{\text{fat}}(\bar{x}_0, \mathbf{v}, \rho) \quad (19)$$

4.4 Fatigue-oriented optimization

The fatigue-oriented unconstrained optimization problem is expressed as follows:

$$\begin{aligned} \min_{\tilde{\mathbf{\Theta}}_{\mathbf{sp}}} \quad & \tilde{J}_{\text{fat}}(\bar{\mathbf{y}}) \\ \text{s.t.} \quad & \bar{\mathbf{y}} = \bar{\mathbf{y}}(\bar{x}_0, \mathbf{v}, \tilde{\mathbf{\Theta}}_{\mathbf{sp}}) \end{aligned} \tag{20}$$

where $\bar{x}_0$ and $\mathbf{v}$ are given. The solution of this optimization problem is thus a function of $\bar{x}_0$ and $\mathbf{v}$. To evaluate the impact of the cost functions on the fatigue cost resulting from the unconstrained optimization, the fatigue cost using the fatigue-oriented optimization and the one using the quadratic optimization are compared.

5. RESULTS

In this section, several preliminary results are presented. First of all, an example of the parametrized quadratic cost function tuning is shown, then the fatigue-oriented optimization solution and the quadratic one are compared on a single disturbance, before being compared on a family of disturbances.
In the sequel, the considered linearized system is derived using the HAWT simulator FAST with the first flapwise mode of the blades activated. It is estimated for wind of 12 m.s^{-1} velocity, without shear nor yaw misalignment, for a collective blade pitch angles of 15.7 degrees. The HAWT simulated is a Senvion MM82, assumed to rotate at rotor nominal speed, i.e. 17.1 rpm. Concerning the discretization, a sample time of 0.1 seconds is considered. For these preliminary results, the disturbance is not actually a wind generated using a standard wind generator, but a gaussian white noise filtered through a first order low pass filter. The low pass filters parameters are its static gain and characteristic time, denoted respectively by K and α. In the sequel, the couples (K, α) are randomly drawn in uniform distributions on the respective intervals $]0, 10^4]$ and $]0, 10]$. The initial condition $\bar{x}_0$ is set to 0 in all simulations.

5.1 Quadratic cost function tuning

In Section 4, it is mentioned that ρ must minimize J_{fat} for given $\bar{x}_0$ and $\mathbf{v}$. Unfortunately, having an analytical expression of J_{fat} as a function of $\bar{x}_0$, $\mathbf{v}$ and ρ is not straightforward, due to the RFC involvement in the fatigue computation and the matrix inversions due to the quadratic cost function optimization problem. Therefore, the brute force method is chosen in order to tune ρ. For given $\bar{x}_0$ and $\mathbf{v}$, 1000 values of ρ are randomly drawn on an uniform distribution, ranging from 10^{-5} to 10^1.
In Fig. 3, the fatigue cost $J_{\text{fat}}(\bar{x}_0, \mathbf{v}, \rho)$ is plotted as a function of ρ, for given $\bar{x}_0$ and $\mathbf{v}$, under a prediction horizon of 100 seconds and for 1000 samples of ρ. The disturbance $\mathbf{v}$ is generated using $K = 6950$ and $\alpha = 2.86$ seconds, these values are randomly generated. In Fig. 4, the same values are plotted, zoomed in the zone of interest. It can be clearly seen that there is a minimum, corresponding approximately to $\rho \simeq 3.4 \times 10^{-2}$. Therefore, the ρ value minimizing J_{fat} for given $\bar{x}_0$ and $\mathbf{v}$ is considered as finely tuned value.

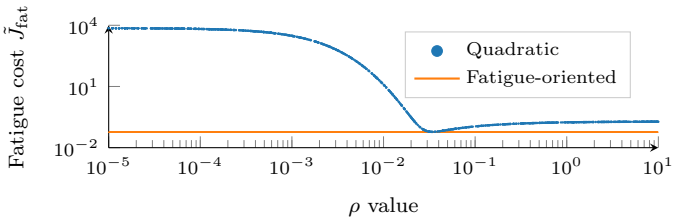

Fig. 3. Scatter plot of $J_{\text{fat}}(\bar{x}_0, \mathbf{v}, \rho)$ in function of ρ and plot of the fatigue cost obtained with the fatigue-oriented optimization. For given $\bar{x}_0$ and $\mathbf{v}$, under a prediction horizon of 100 seconds and for 1000 values of ρ.

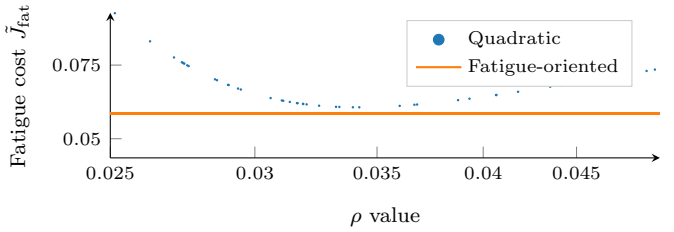

Fig. 4. Scatter plot of $J_{\text{fat}}(\bar{x}_0, \mathbf{v}, \rho)$ in function of ρ and plot of the fatigue cost obtained using the fatigue-oriented optimization. For given $\bar{x}_0$ and $\mathbf{v}$, under a prediction horizon of 100 seconds and zoomed in the zone of interest.

5.2 Comparison on a single disturbance

This finely tuned value of ρ is used to compare the consequence on the closed-loop fatigue when using the two following candidate optimization problems:

(1) The finely tuned unconstrained quadratic cost (18).
(2) The unconstrained fatigue-oriented cost (20).

The fatigue-oriented optimization allows to obtain a lower fatigue cost than the finely tuned quadratic one, with respective fatigue cost of 5.75×10^{-2} and 5.95×10^{-2}. It means that the fatigue-oriented optimization allows a relative 3.4% reduction in fatigue cost compared to the finely tuned quadratic one.
In Fig. 5, the finely tuned quadratic and the fatigue-oriented optimizations solutions time series are plotted. It can be seen that the $\theta_{yaw,sp}$ solutions are very close for both optimization. However, it can be seen the $\theta_{tilt,sp}$ fatigue-oriented solution is more active than the quadratic one, which makes the difference in terms of fatigue cost. Comparing the optimizations solution on a single disturbance clearly advantage the finely tuned quadratic optimization, because the tuning is made on the same disturbance it is tested on, which is obviously not realistic. This comparison emphasizes that the fatigue-oriented optimization is already slightly better. To show the ability of the optimizations to adapt in various conditions, the two fatigue cost of the optimizations solutions are compared under a family of disturbances.

5.3 Comparison on a family of disturbances

In this family of disturbances, each disturbance is defined by a couple (K, α), randomly drawn in previously mentioned distributions. For each disturbance, the same

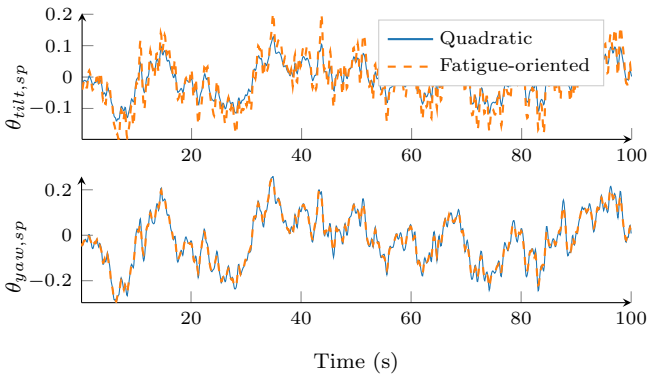

Fig. 5. Plot of the solution found by the finely tuned quadratic and fatigue-oriented optimizations.

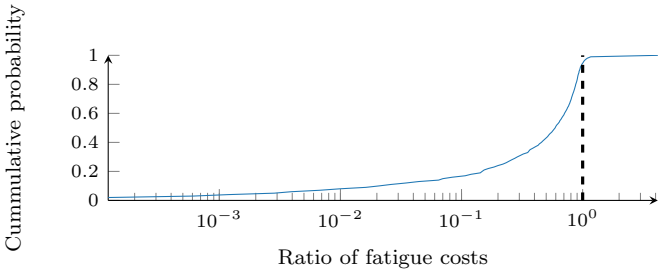

Fig. 6. Cumulative probability distribution of the fatigue costs ratio obtained from 1000 samples.

finely tuned quadratic cost (with $\rho \simeq 3 \times 10^{-2}$) and the same fatigue-oriented cost functions ($(a, b) = (2.6, 4.6)$ for $m = 4$ and $(a, b) = (5.6, 15.6)$ for $m = 10$) are used for the optimizations on every disturbances generated. Each disturbance yields thus two fatigue costs, one for the quadratic optimization solution and the other for the fatigue-oriented one.

In Fig. 6, the cumulative probability distribution of the relative fatigue cost between the fatigue-oriented optimization solution and the quadratic one is plotted. It can be seen that the probability that the fatigue-oriented optimization solution allows to yield a lower fatigue cost than the quadratic one is greater than 0.94. Moreover, the probability that the relative fatigue would increase more than 10% is lower than 0.02, while the probability that the fatigue-oriented cost function would decrease the fatigue cost more than 50% is greater than 0.56. Therefore, it can be claimed that the use of the fatigue-oriented cost function can allow sensitive fatigue reductions, and is robust on this family of disturbances, compared to the considered ensemble of quadratic cost functions.

6. CONCLUSION AND PERSPECTIVES

In this paper, a novel fatigue-oriented cost function is presented in order to optimize the fatigue trade-off of a HAWT. It is compared to an ensemble of quadratic cost functions under a family of disturbances. Preliminary results suggest that the fatigue-oriented cost function can sensitively reduce the fatigue cost trade-off. It should be noticed that several assumptions were made as the Goodman correction is neglected which can be questioned, and should realistic disturbances be considered. Comparison is done with a reduced-dimensional parametrization of quadratic cost functions. Moreover, linear model is considered for the underlying dynamics. Consequently, further investigation are still needed in order to confirm the results of the present work. The ultimate goal being to compare the control resulting from this optimization on a realistic HAWT simulator under turbulent winds, against state-of-the-art fatigue-oriented control techniques.

REFERENCES

Barradas-Berglind, J. and Wisniewski, R. (2016). Representation of fatigue for wind turbine control. *Wind Energy*, 19, 2189–2203.

Biegel, B. (2011). Distributed control of wind farm. *MSc Theses*.

Bir, G. (2008). Multi-blade coordinate transformation and its application to wind turbine analysis. In *Proc. 46th AIAA aerospace sciences meeting and exhibit*, 1300.

Bossanyi, E. (2003). Individual blade pitch control for load reduction. *Wind Energy*, 6, 119–128.

Coleman, R.P. and Feingold, A.M. (1957). Theory of self-excited mechanical oscillations of helicopter rotors with hinged blades. *National Advisory Committee for Aerounautics*.

Collet, D., Di Domenico, D., Sabiron, G., and Alamir, M. (2019). A data-driven approach for fatigue-based individual blade pitch controller selection from wind conditions. In *2019 American Control Conference (ACC)*, 3500–3505. IEEE.

de Jesus Barradas-Berglind, J., Wisniewski, R., and Soltani, M. (2015). Fatigue damage estimation and data-based control for wind turbines. *IET Control Theory & Applications*, 9, 1042–1050.

Downing, S.D. and Socie, D. (1982). Simple rainflow counting algorithms. *International journal of fatigue*, 4, 31–40.

GWEC (2016). Global wind energy outlook. Technical report, Global Wind Energy Council.

GWEC (2018). Global wind report. Technical report, Global Wind Energy Council.

Hammerum, K., Brath, P., and Poulsen, N.K. (2007). A fatigue approach to wind turbine control. *Journal of Physics: Conference Series*, 75, 012081.

Hansen, M.O. (2015). *Aerodynamics of wind turbines*. Routledge.

Hayman, G. (2012). Mlife theory manual for version 1.00. Technical report, National Renewable Energy Laboratory.

Jonkman, J., Butterfield, S., Musial, W., and Scott, G. (2009). Definition of a 5-MW reference wind turbine for offshore system development. Technical report, National Renewable Energy Laboratory.

Knudsen, T., Bak, T., and Svenstrup, M. (2015). Survey of wind farm control—power and fatigue optimization. *Wind Energy*, 18, 1333–1351.

Loew, S., Obradovic, D., and Bottasso, C. (2019). Direct online rainflow-counting and indirect fatigue penalization methods for model predictive control. In *Proc. European Control Conference (ECC)*, 3371–3376.

Miner, M. (1945). Cumulative damage in fatigue. *Journal of Applied Mechanics*, 3, 159.

Palmgren, A. (1924). Die lebensdauer von kugellagern. *Zeitshrift des Vereines Duetsher Ingenieure*, 68, 339.